Journal of Manufacturing Processes 48 (2019) 210–217

Contents lists available at ScienceDirect

Journal of Manufacturing Processes

journal homepage: www.elsevier.com/locate/manpro

Virtual reality human-robot collaborative welding: A case study of weaving gas tungsten arc welding

Qiyue Wang[a,b], Yongchao Cheng[b,c], Wenhua Jiao[a,b], Michael T. Johnson[a], YuMing Zhang[a,b,*]

[a] Department of Electrical and Computer Engineering, University of Kentucky, Lexington, KY, 40506, USA
[b] Institute for Sustainable Manufacturing, University of Kentucky, Lexington, KY, 40506, USA
[c] Welding Research Institute and Engineering Research Center of Advanced Manufacturing Technology for Automotive Components-Ministry of Education, Beijing University of Technology, Beijing, 100124, PR China

ARTICLE INFO

Keywords:
Human-robot collaboration
Virtual reality
Cyber-physical system
Seam tracking
Weaving welding

ABSTRACT

To combine the advantages of humans (adaptive intelligence) and robots (higher movement accuracy and physical limitation), we propose a virtual reality human-robot collaborative welding system which allows them to collaborate with each other to complete welding tasks. A common welding method, weaving gas tungsten arc welding (GTAW) is presented as a case study. In this system, a 6-degree of freedom (6-DoF) robot UR-5 carrying the welding torch works as the final performer of weaving welding. A virtual welding environment based on HTC VIVE is built where humans can observe the working scene via a motion-tracked headset without being onsite physically. A mapping model between arc voltage, arc length and welding current is established, and based on this model a seam tracking algorithm is developed which allows the robot to track the weld seam automatically. The robot is pre-programmed to weave the welding torch across the weld seam. The robot travelling along the weld seam is fully controlled by the human operator via motion-tracked handle per the observed working scene. This teleoperation style allows the humans to adjust the travel speed adaptively and freely as needed without suffering onsite danger. The proposed collaborative welding system combines the advantages of humans and robots together, utilizing the intelligence and adaptability of the human operator with precise movement obtained from robots. The welding experiments show that the welded workpiece from human-robot collaboration has better performance compared with that from either humans or robots separately and demonstrated the effectiveness of the proposed virtual reality human-robot collaborative welding system.

1. Introduction

Welding plays an extreme important role in industrial manufacturing. In most practical applications, welding robots and welding operators are the two main performers of welding tasks. Compared with humans, robots have higher movement precision, stability and fewer physical limitations due to the environmental hazards of vacuum, pressure, temperature, radiation, poison and fatigue. Several different welding methods, including spot welding, stud welding, arc welding, and laser welding, have been successfully robotized to increase production efficiency [1]. According to the International Federation of Robotics (IFR), the percentage of tasks accomplished by welding robots is now over 50% in industrial robots [2]. However, current welding robots are pre-programmed and are only effective in a highly structured working environment. These welding robots can execute pre-defined actions taught by robot programmers or generated from off-line programming which does not perform well when facing unpredicted disturbances due to workpiece variation, bad assembling, or other common factors which occur in an industrial setting. In order to produce high-quality weld joints under disturbance, sensors such as ultrasonic sensors [3,4], arc sensors [5,6], thermal sensors [7,8], audio sensors [9,10] and vision sensors [11–15] have been applied to monitor and control welding processes in real time. In these works, the first step is typically to identify and extract features to characterize the weld joint penetration status. After this, control algorithms are developed and applied to make sure that the weld joints are in full penetration status which is a critical factor determining the mechanical properties of weld joints such as strength, anti-corrosion ability and service life. However, these sensing and control methods have not been applied widely due to the several key weaknesses. Feature information is often not accurate due to the inevitable disturbances from irregular arc variation, intensive arc radiation, sound noise, electromagnetic interference and

* Corresponding author at: Department of Electrical and Computer Engineering, University of Kentucky, Lexington, KY, 40506, USA.
E-mail addresses: qiyue.wang@uky.edu (Q. Wang), yongchao.cheng@uky.edu (Y. Cheng), wenhua.jiao@uky.edu (W. Jiao), mike.johnson@uky.edu (M.T. Johnson), yuming.zhang@uky.edu (Y. Zhang).

https://doi.org/10.1016/j.jmapro.2019.10.016
Received 4 July 2019; Received in revised form 30 September 2019; Accepted 3 October 2019
Available online 15 November 2019

other factors. In addition, the welding process models built are not accurate due to the complexity of the welding processes which are nonequilibrium physiochemical processes with metal heating, melting and solidifying locally with weld beads formed via complex heat-mechanics-metallurgy coupling reactions. Furthermore, due to the intrinsic dynamics, non-linearity, time variance of welding processes, it is also hard to design proper control algorithms. These three weaknesses have severely limited the wide applications of full intelligent welding robots in practical manufacturing.

In comparison, skilled welding operators (human welders) can perform well in spite of working disturbance by adjusting welding torch movement adaptively after perceiving, analyzing and integrating information from welding processes [16]. This is the reason why skilled human welders are usually the performers for critical welding applications. Moreover, human welders have higher flexibility and therefore are often preferred for small-volume and unstructured welding applications considering the cost both in time and capital investment. However, humans are exposed to hazardous fumes, gas and arc radiation when undertaking welding tasks on site [17,18]. They also have lower performance in accurate, repeated long-term control of welding torch movement than welding robots. In addition, according to American welding society (AWS) there is an urgent global shortage of skilled welders [19]. Since humans and robots have unique advantages and disadvantages, combining these advantages could help address these multiple issues. To accomplish these, a virtual reality human-robot collaborative welding system has been developed and a common welding method, weaving GTAW, is presented as a case study. In this novel collaborative system, the human operator is responsible for controlling the welding torch to travel along weld seam per the observed welding scene. This is the most challenging issue which current welding robots cannot address perfectly, and the intelligence and adaptability demonstrated is also the main criterion to evaluate the skill level of human welders. The welding torch trajectory planning and movement (weaving across weld seam in our application) is done by robots since robots have higher movement accuracy, better stability and durability than humans. The essential problem for welding robot trajectory planning and movement is seam tracking i.e. the robots need the ability to modify the trajectory when the weld seam deviates from the intended plan. Some sensing methods have been proposed to achieve this goal including arc sensing [20,21], vision sensing [22,23], ultrasonic sensing [24], electromagnetic sensing [25], infrared sensing [26] and tactile sensing [27]. By using these sensing methods, the characteristic information is extracted, and the seam position is identified further. The robots adjust their trajectories if the deviation exists. Among all these sensing methods, only arc sensing does not need additional sensors since they are usually embedded in welding power supplies, which reduces the system complexity and cost. In addition, collecting the arc voltage and welding current data by arc sensors does not create any disturbance and has the highest robustness among all sensing methods. To accomplish seam tracking based on arc sensors, seam deviation is computed by arc length dynamics using a mapping model of arc length and arc information. This is only effective in grooved workpieces and the electrodes need to scan across weld seams to collect the arc length data. Based on this principle, some seam tracking systems have been developed and applied in gas metal arc welding (GMAW) by rotating decentered torches [20,21,28,29].

However, this approach is not effective in GTAW where tungsten electrodes are much more rigid than the filler wire electrode in GMAW and cannot be deformed. Therefore, the arc sensors are only used in height tracking for GTAW instead of seam tracking [30]. We thus focus on application of our new collaborative welding method to weaving GTAW applications where tungsten electrode is weaved across seams time-harmonically by a 6-DoF robot which addresses this issue.

As the most challenging part in welding, adaptive travel speed adjustment of welding torch along the weld seam is done by a human operator. To protect the humans from hazardous agents generated in welding manufacturing, the robot travelling along weld seam is fully controlled by human via a virtual reality (VR) welding environment. VR is an innovative interface for human-machine interaction and has been playing a growing role in many industrial applications, including the transition of manufacturing to Industry 4.0 particularly [31,32]. By affording the fast-visualized evaluation, VR has been used for product design [33–35] and applied in the area of assembling tools [36], airplane [37], construction [38] and automotive [39,40]. Skill training for novices is another application of VR in manufacturing [41–43]. By observing and responding to the computer-generated virtual environment, trainees are evaluated based on their operations and learn the skill without conducting practical manufacturing on site such that the training safety is increased, and training cost is reduced. Some specific virtual training systems have been developed to some manufacturing processes used widely in industry, including welding [44], casting [45], painting [46], construction [47] and mining [48]. Current VR research focuses on the pre-manufacturing stage. In this paper, we extend VR to practical manufacturing environments as an interface for human operators to accomplish tasks in hazardous environments.

This paper introduces a virtual reality human-robot collaborative welding system, with weaving GTAW presented as a case study. By using VR hardware as the interface, a virtual welding system is built where the humans and the robots can collaborate with each other. In such a system, the robots perform the final welding tasks with automatic weaving across and tracking of the welding seam since they have higher movement accuracy and physical limitation. Robot travelling along the weld seam is fully controlled by the human welder who possesses adaptive intelligent adjustment ability to minimize the negative effect from the variable and unpredicted working environment. Via this proposed virtual reality human-robot collaborative welding system, both the advantages of the humans (adaptive intelligence) and robots (higher movement accuracy and physical limitation) are combined. This human-robot collaboration framework based on VR can be extended to other similar manufacturing processes requiring professional skills such as additive manufacture, spraying and painting. The details of system configuration are presented in Section 2. Section 3 discusses the principles of human-robot collaborative weaving welding. Welding experiments are conducted, and the results are analyzed in Section 4. The conclusions and future work are summarized in Section 5.

2. System configuration

As shown in Fig. 1, the proposed virtual reality human-robot collaborative welding system is a cyber-physical system (CPS) where humans and robots can collaborate to complete welding tasks. A virtual welding environment based on costumer-grade VR hardware, the HTC VIVE system, is implemented. The UR-5 robot carries the welding torch and works as the final welding performer. Welding continues with power supplied from a Liburdi Pulsweld P200 which incorporates embedded arc sensors to sense the arc voltage and welding current in real time. V-grooved workpieces whose geometrical cross profile is shown in Fig. 2 are welded using the parameters in Table 1. The field information during welding especially the weld pool information should be presented for the human perceiving the welding process and making next decisions. Some modern analytical models have been developed to offer the temperature distribution information [49–52] which is critical to determine the welding quality. However, temperature distribution may be too complex for human to respond and analytical models are built based on some assumptions, such as relatively flat work-piece surface, while many welding tasks are more complex, for example in this study the work-pieces are grooved. Therefore, an industrial camera (Point Grey FL3FW03S1C) with bandpass optical filter is applied to capture the visible working scene in real time. The details of the filter and the configuration of the camera are shown in Table 2. The images captured are transmitted to the computer via IEEE-1394 interface.

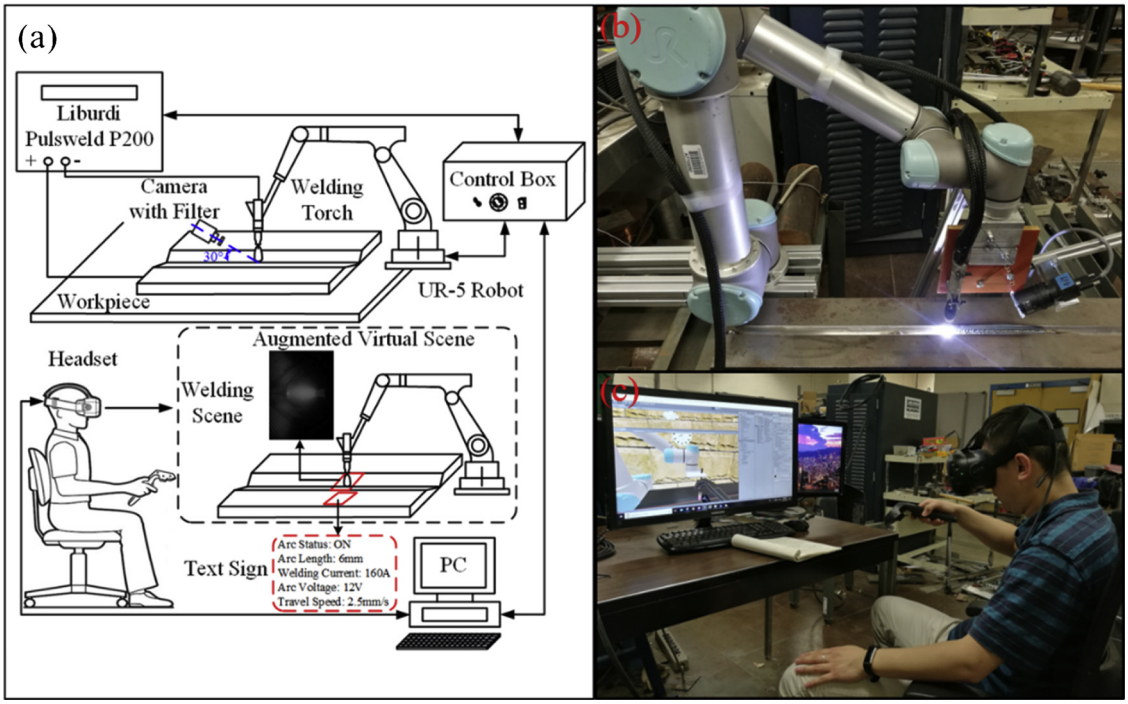

Fig. 1. System configuration of virtual reality human-robot collaborative welding system (a) Schematic diagram (b) robot welding onsite (c) human controlling robot remotely using VR head-mounted display.

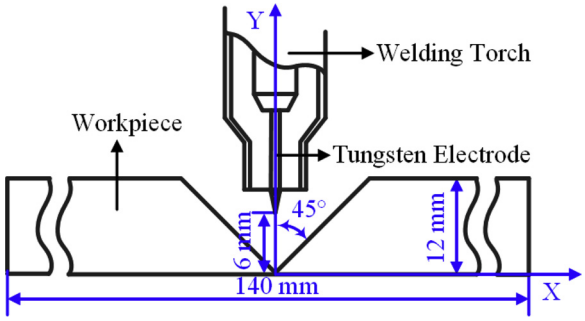

Fig. 2. Geometrical cross section of the welded workpiece.

Table 1
Welding Parameters Applied.

Welding Parameters	Value
Welding Type	DCEN
Welding Current (A)	140-180
Travel Speed (mm/s)	1.8
Tungsten Diameter (mm)	2.4
Tungsten Grind Angle (°)	30
Shielded Gas	Argon
Gas Flow (SCCM)	5600
Workpiece Material	DH36
Weaving Type	Sinusoid
Weaving Amplitude (mm)	2
Weaving Period (s)	2

Table 2
Camera Configuration Applied.

Configuration	Value
Filter Center (nm)	650 ± 2
Filter FWHM (nm)	10 ± 2
Image Size (Pixel)	640 × 480
Format	Mono8
Frame Rates (FPS)	30
Shutter Time (s)	0.03
Sharpness	3000
Gain	0
Gamma	2.5

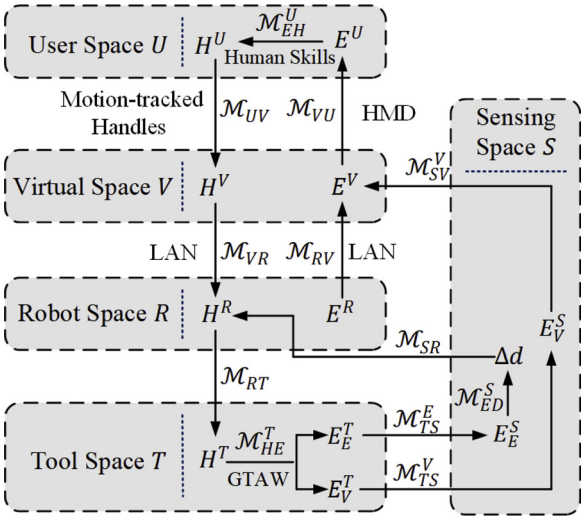

Fig. 3. Cyber-physical model of virtual reality human-robot collaborative welding.

3. Principles of VR human-robot collaborative welding

3.1. Cyber-physical model

The cyber physical model of the virtual reality human-robot collaborative welding is shown in Fig. 3. Five spaces including user space *U*, virtual space *V*, robot space *R*, tool space *T* and sensing space *S* co-exist and the information flows among them. In one working cycle, the

human operator observes the augmented working scene E^U and makes the intelligent response H^U to ensure that welding continues in a desired state by adjusting travel speed adaptively in user space U. The mapping model $\mathcal{M}_{EH}^U$ from E^U to H^U characterizes the human welder skills. Via the motion tracked handles, H^U is mapped as H^V charactering the movement of the virtual torch in virtual space V. The robot receives H^V via local area network (LAN) as the commanded pose and moves its joints after inverse kinematics computation. The movement of welding torch is attached in this robot and GTAW maintains modeled as $\mathcal{M}_{HE}^T$ mapping welding parameters H^T to electrical information ${E_E}^T$ and visual information ${E_V}^T$. The electrical information ${E_E}^T$ includes arc voltage and welding current sensed by the arc sensors. The position difference between the tungsten electrode and weld seam Δd is computed and the robot adjusts the weaving center to track the weld seam. The visual information is the welding scene captured by the camera and transmitted to virtual space where it is integrated with robot information E^R to generate a 3D augmented virtual welding environment E^V. The human observes the 3D virtual welding environment E^V via motion-track headset and continues the next working cycle. The entire system is developed in Unity 3D and programmed with C# language.

3.2. Robotic weaving and seam tracking

The welding torch weaving and automatic seam tracking are done by the robot. The weaving movement has sinusoid trajectory with pre-programmed weaving center and amplitude. The automatic seam tracking is adaptive and model driven, based on the principle that arc voltage depends on arc length and welding current. The first task is to model the mapping function $U = U(L, I)$ where U is arc voltage, I is the welding current and L is the arc length. Using the welding parameters in Table 1, weaving welding is conducted and welding current, arc length and arc voltage data are collected. The diagrams of arc voltage varying with welding current and arc length are shown in Fig. 4(a) and (b) respectively. It can be seen that both welding current and arc length affect arc voltage linearly when the other factor is fixed such that we have:

$$\frac{\partial U(L,\ I)}{\partial L} = f(I)\# \tag{1}$$

$$\frac{\partial U(L,\ I)}{\partial I} = g(L)\# \tag{2}$$

where $f(I)$ and $g(L)$ are the single-variable function of I and L. From Eqs. (1) and (2), it can be derived:

$$\frac{\partial^2 U(L,\ I)}{\partial L \partial I} = \frac{df(I)}{dI} = \frac{dg(L)}{dL} = Contant\# \tag{3}$$

The general solution for Eq. (3) is:

$$U(I, L) = k_0 IL + k_1 I + k_2 L + k_3\# \tag{4}$$

The unknown parameters in Eq. (4) are identified using the least squares method. Curve fitting results are shown in Table 3 and Fig. 4(c). From the fitting results, the $R^2 = 0.9265$ is close to 1 and p-value is 0 which is much smaller than the default significance level of 0.05 used commonly in engineering. Therefore, the proposed model has statistical significance which verifies the validity of hypothesis among arc voltage, welding current and arc length.

As shown in Fig. 5, the relative position of weaving center to weld seam determines the arc length distribution during weaving welding, and the relative deviation between them Δd can be computed by the arc length difference ΔL at weaving boundary position and further computed by arc voltage difference ΔU:

$$\Delta d = \frac{1}{2tan\theta}\Delta L = \frac{1}{2tan\theta}\cdot\frac{\Delta U}{k_0 I + k_2}\# \tag{5}$$

By Eq. (5), Δd can be identified by arc voltage and welding current directly which are both available from arc sensors. The flowchart of the developed automatic seam tracking algorithm is shown in Fig. 6. In each weaving cycle, the boundary position in weaving direction (y-axis in our application), Y_{max} and Y_{min} are found and the corresponding arc

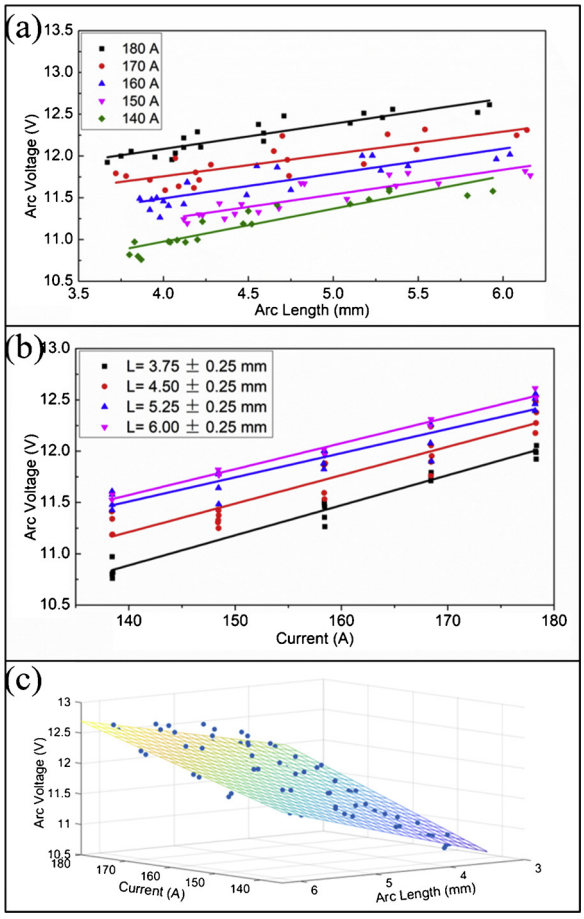

Fig. 4. Fitting for $U = U(L, I)$ (a) L determines U linearly (b) I determines U linearly (c) Fitting curve of $U = U(L, I)$.

Table 3
Fitting Results of $U = U(L, I)$.

Parameters	Value
k_0 (Ω/mm)	−0.002
k_1 (Ω)	0.0359
k_2 (V/mm)	0.641
k_3 (V)	4.591
R^2	0.9265
F-statistic	403.2865
p-value	0

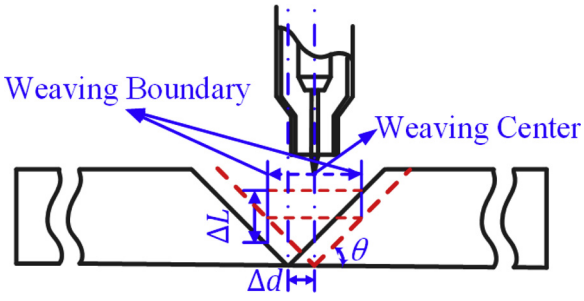

Fig. 5. Weaving center deviation from weld seam results in asymmetric arc length distribution.

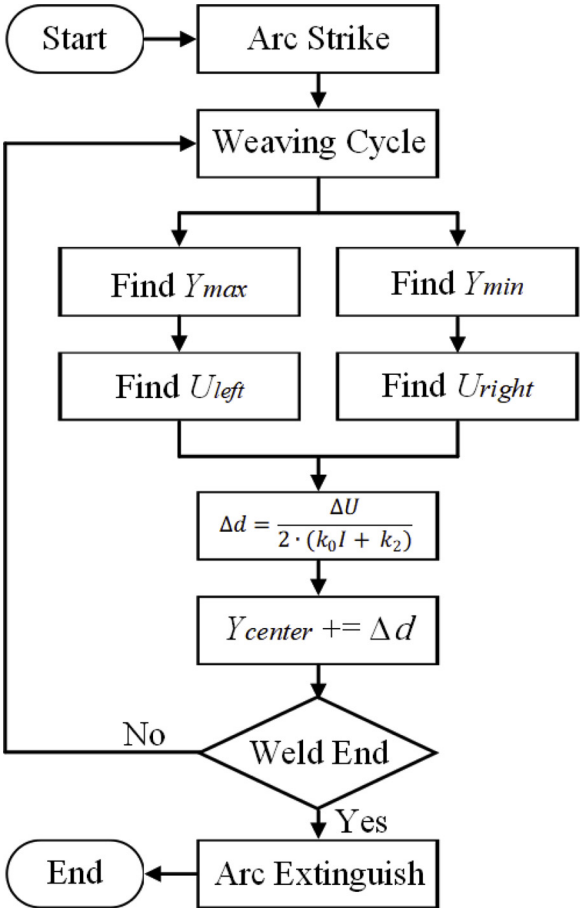

Fig. 6. Working flowchart of proposed automatic seam tracking algorithm.

voltage, U_{left} and U_{right} are measured. Then the seam deviation Δd is identified using Eq. (5). The robot adjusts the weaving center by Δd to track the weld seam again if deviation exists.

3.3. Manual speed adjustment

A virtual welding environment is built based on HTC VIVE VR system which the human operator is immersed in and interacts with. In this virtual welding environment, the 3D models of rigid objects in virtual welding environment such as the robot, the welding torch and workpieces are pre-built, and their spatial position and orientation are configurated based on that in real welding environment. Specifically, the duplicated 3D models with same gematrical dimension are pre-build using computer-aided design (CAD) software and initialized in the virtual environment with the same position and orientation as that at the welding site. When the welding started, the rotation degree of each joint of the robot is acquired and corresponding joints of virtual robot rotate the same degree such that the virtual robot can follow the pose of the real robot in real time. The deformable objects in virtual welding environment such as arc and weld pool are rendered by capturing and projecting the images of corresponding real objects. The human operator observes the 3D virtual welding scene by head-mounted display (HMD) where the observed scene is the 2D projection of the 3D virtual environment on the viewing plane which can be identified by the motion-tracked headset. A typical observed scene contains two kinds of information, base visual information plus augmented data, as shown in Fig. 7. The base information is visual information human observes as if they were physically on-site, including the robot, welding torch, workpiece, arc, and weld pool. The other information is augmented information which is sensed by sensors and displayed as text, such as

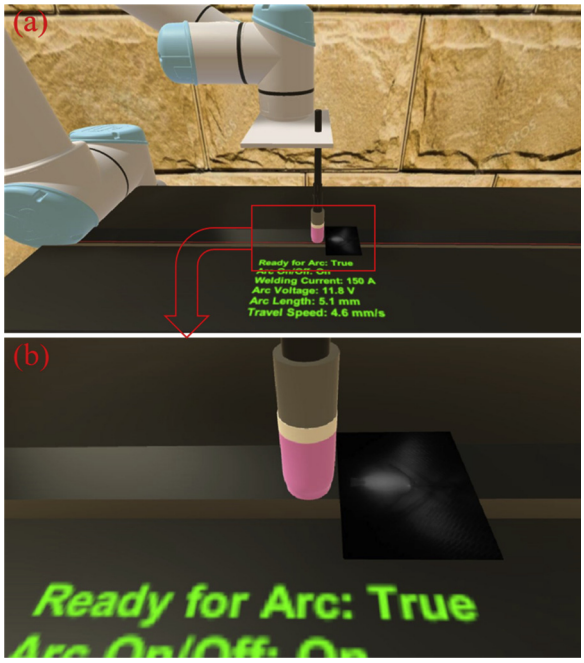

Fig. 7. A typical working scene shown to human by HMD (a) global view (b) local view.

welding current, arc length, arc voltage and instantaneous travel speed. This augments the perception of the operator with information that is typically unavailable to human welders in conventional manual welding. After observing augmented welding scene, the human operator controls the movement of the robot along the weld seam by motion-tracked handles.

4. Welding experiments and analysis

Experiments including robotic welding, manual welding and human-robot collaborative welding are conducted to verify the effectiveness of the proposed human-robot collaborative welding system.

4.1. Robotic welding

Using the welding parameters in Table 1, fully robotic weaving welding is done without any human operators involved. The robot is pre-programmed with the proposed automatic seam tracking algorithm applied. To mimic the unpredicted disturbances in practical working environment, two kinds of artificial disturbances are added. Noise welding current within ± 20A taking 10A as a step is added in the desired welding current 160A to mimic inconsistent welding conditions. An artificial deviation degree θ between travel direction and weld seam is configurated to mimic the practical seam deviation as shown in Fig. 8. The travel speed of welding torch along weld seam is 1.8 mm/s. The weaving trajectory with automatic seam tracking is shown in Fig. 9(a) and the welded workpiece is shown in Fig. 9(b). As shown in Fig. 9(b), the inconsistent welding current generates inconsistent weld bead, especially, the incomplete fusion happens when the welding current is low (stage II and III). This inconsistence in weld bead verifies

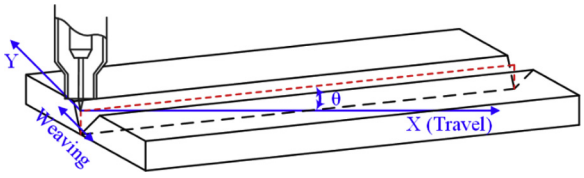

Fig. 8. Welding torch travel direction deviates the weld seam with degree θ.

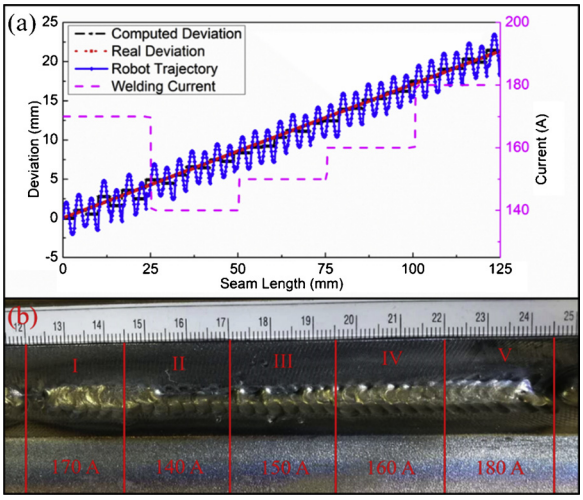

Fig. 9. Robotic welding (a) robot trajectory (b) welded workpiece.

that the artificial disturbances are effective in affecting the weld joints negatively.

4.2. Manual welding

Using the same experimental configuration in robotic welding, manual welding is done by the human operator observing the working scene. All components of weaving welding including weaving welding torch, seam tracking and intelligent speed adjustment are done by the operator and the robot simply copies the horizontal trajectories from the human with the vertical position and orientation fixed. The demonstrated weaving trajectory across weld seam, travel speed along weld seam and the welded workpiece are shown in Fig. 10. The raw travel speed data shown in Fig. 10(b) has a large fluctuation which increases the difficulty of recognizing the intended travel speed. Therefore, the time-averaged data is presented for a clearer demonstration. The time averaged speed is computed as the mean travel speed in the interval before and after 1s:

$$\overline{v_t} = \frac{\sum_{i=-10}^{10} v_{t+0.1i}}{21} \# \tag{6}$$

From the operation data in Fig. 10, the human operator adjusts the travel speed adaptively faced with the artificial disturbance and more consistent weld bead is obtained compared with that from robotic welding. However, due to the instability and inaccuracy in manual movement, which is the intrinsic physical limitation of humans, the weaving amplitudes are not consistent and fluctuate around desired ones (2 mm) as shown in Fig. 10(a).

4.3. Human-robot collaborative welding

With the same experimental configuration used previously, human-robot collaborative welding is done. As discussed in Section 3, the robot carrying the welding torch weaves across and tracks the weld seam automatically. The human operator observes the working scene and adjusts the travel speed adaptively. The robotic weaving trajectory with automatic seam tracking is shown in Fig. 11(a). The travel speed applied from human and welded workpiece from human-robot collaborative welding are shown in Fig. 11(b) and (c), respectively. With the proposed seam tracking algorithm, the robot weaves the welding torch across weld seam with desired trajectory even the deviation exists. The movement of welding torch along the weld seam is adjusted adaptively by the human operator such that a consistent weld bead is obtained.

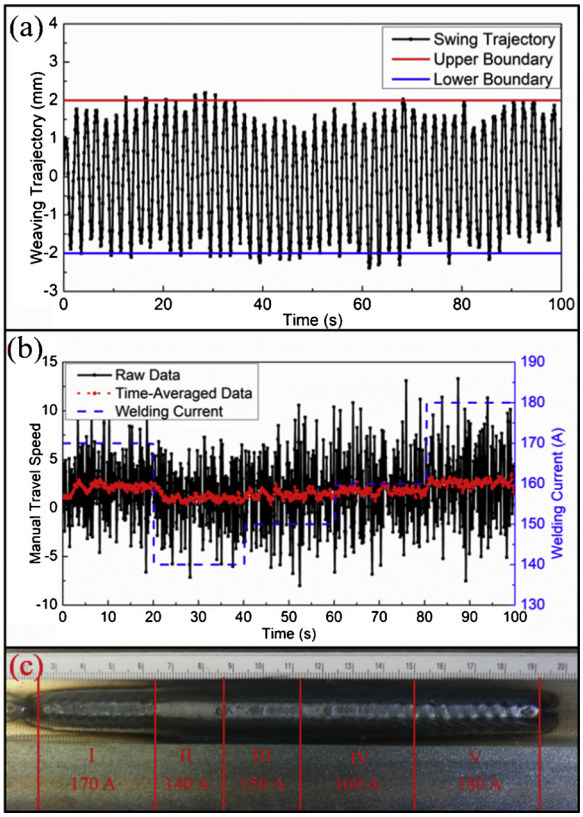

Fig. 10. Manual welding (a) weaving trajectory (b) travel speed demonstrated (c) welded workpiece.

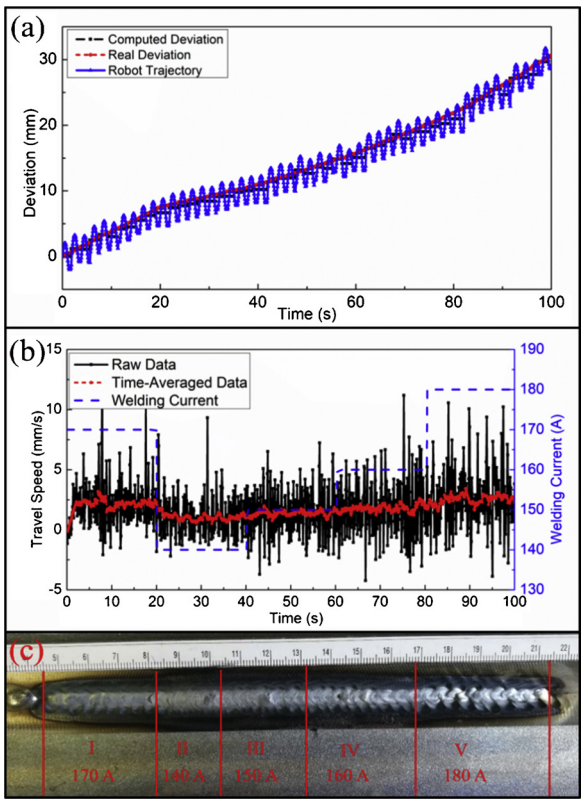

Fig. 11. Human-robot collaborative welding (a) weaving trajectory (b) travel speed (c) welded workpiece.

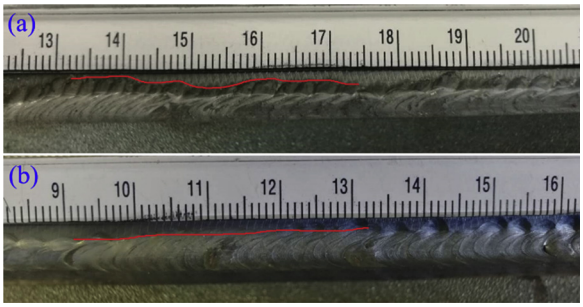

Fig. 12. The solid red line shows the outline of weld bead (a) from manual welding (b) from human-robot collaborative welding. (For interpretation of the references to colour in this figure legend, the reader is referred to the web version of this article).

Table 4
Comparation of Manual Weaving and Robotic Weaving.

Quantity	Manual	Robotic
Weaving Amplitude Mean	1.8112 mm	2.0 mm
Min Weld Width	7.0 mm	8.0 mm
Max Weld Width	9.0 mm	8.5 mm
Width Inconsistency	2.0 mm	0.5 mm

4.4. Result analysis

In purely robotic welding, the computed deviation tracks the real deviation well such that the weaving welding can track the weld seam well, even in a large deviation working environment (up to 20 mm deviation with 125 mm seam length) as shown in Fig. 9. However, the robot cannot adjust the travel speed when faced with a disturbance to the working environment, which results in the inconsistent welding quality. In contrast, as shown in Fig. 10, the human operator can adjust travel speed adaptively by observing the working scene. The human increases the travel speed when welding current increases such that the heat input to the workpiece is relatively constant and the weld bead has consistent appearance. This demonstrates the advantages of human welders in practical welding. However, human operators are not good at repeated and accurate movement. As shown in Fig. 10(a), the amplitude of the manual weaving trajectory from the human operator is not constant. This results in an inconsistent width of the weld bead. The human-robot collaborative welding overcomes the individual disadvantages of humans and robots. By using robotic weaving with automatic seam tracking, the human-robot collaborative welding inherits the advantages from robotic welding and overcomes the disadvantages from manual welding i.e. inaccurate weaving and working fatigue. As shown in Fig. 12 and Table 4, manual weaving results in an inconsistency of 2 mm in the weld width, ranging between 7 mm and 9 mm. In human-robot collaborative welding, this inconsistency is reduced from 2 mm to 0.5 mm, due to robotic weaving which can offer more stable and accurate movement, while the collaboration from the human also assures the adaptation capability similarly as in manual welding. The travel speed is adjusted by the operator such that a consistent weld bead is obtained as shown in Fig. 11. Therefore, the human-robot collaborative welding system combines the advantages of manual welding and robotic welding and the welded workpiece has better performance than that accomplished by either a human operator or a robot individually.

5. Conclusions and future work

This paper has introduced a virtual reality human-robot collaborative welding system and applied this system in weaving gas tungsten arc welding as a case study. The welding torch is installed in UR-5 robot with weaving movement across weld seam and automatic seam tracking. A virtual welding environment is generated for the human operator to observe the working scene and respond to unpredicted disturbance by adaptively adjusting the travel speed along weld seam remotely as needed. Using the proposed collaborative welding system, the individual advantages of humans and robots are combined, as demonstrated by the improved performance achieved in the presented GTAW experiments. In addition, the use of the VR interface significantly increases safety and reduces environmental hazards to the human operators and augments the perception of the human operator for welding processes. The virtual reality human-robot collaboration framework developed here is flexible and can easily be extended to other similar manufacturing processes which would benefit from combining human adaptability and robotic precision.

Future work will focus on the impact of human-robot collaborative operations on mechanical properties and microstructures in different welding processes. The mapping model between the observed working scene and the reaction behavior of human welders will also be explored.

Declaration of Competing Interest

The authors declare that they have no known competing financial interests or personal relationships that could have appeared to influence the work reported in this paper.

The authors declare the following financial interests/personal relationships which may be considered as potential competing interests.

References

[1] Ogbemhe J, Mpofu K. Towards achieving a fully intelligent robotic arc welding: a review. Ind Rob 2015;42(5):475–84. https://doi.org/10.1108/IR-03-2015-0053.
[2] Sprovieri J. New technology for robotic welding. 2016 Available: https://www.assemblymag.com/articles/93555-new-technology-for-robotic-welding.
[3] Graham GM, Ume IC. Automated system for laser ultrasonic sensing of weld penetration. Mechatronics 1997;7(8):711–21. https://doi.org/10.1016/s0957-4158(97)00031-7.
[4] Mi B, Ume C. Real-time weld penetration depth monitoring with laser ultrasonic sensing system. J Manuf Sci Eng 2006;128(1):280–6. https://doi.org/10.1115/1.2137747.
[5] Li XR, Shao Z, Zhang YM, Kvidahl L. Monitoring and control of penetration in GTAW and pipe welding. Weld J 2013;92(6):190–6.
[6] Wang Z, Zhang Y, Wu L. Adaptive interval model control of weld pool surface in pulsed gas metal arc welding. Automatica 2012;48(1):233–8. https://doi.org/10.1016/j.automatica.2011.09.052.
[7] Chandrasekhar N, Vasudevan M, Bhaduri AK, Jayakumar T. Intelligent modeling for estimating weld bead width and depth of penetration from infra-red thermal images of the weld pool. J Intell Manuf 2015;26(1):59–71. https://doi.org/10.1007/s10845-013-0762-x.
[8] Wikle HC, Kottilingam S, Zee RH, Chin BA. Infrared sensing techniques for penetration depth control of the submerged arc welding process. J Mater Process Technol 2001;113(1):228–33. https://doi.org/10.1016/S0924-0136(01)00587-8.
[9] Lv N, Zhong J, Chen H, Lin T, Chen S. Real-time control of welding penetration during robotic GTAW dynamical process by audio sensing of arc length. Int J Adv Manuf Technol 2014;74(1–4):235–49. https://doi.org/10.1007/s00170-014-5875-7.
[10] Lv N, Xu Y, Li S, Yu X, Chen S. Automated control of welding penetration based on audio sensing technology. J Mater Process Technol 2017;250:81–98. https://doi.org/10.1016/j.jmatprotec.2017.07.005.
[11] Zhang YM, Kovacevic R, Li L. Characterization and real-time measurement of geometrical appearance of the weld pool. Int J Mach Tools Manuf 1996;36(7):799–816. https://doi.org/10.1016/0890-6955(95)00083-6.
[12] Ma X, Zhang Y. Gas metal arc weld pool surface imaging: modeling and processing. Weld J 2011;90(5):85–94.
[13] Song HS, Zhang YM. Three-dimensional reconstruction of specular surface for a gas tungsten arc weld pool. Meas Sci Technol 2007;18(12):3751–67. https://doi.org/10.1088/0957-0233/18/12/010.
[14] Liu YK, Zhang YM. Model-based predictive control of weld penetration in gas tungsten arc welding. IEEE Trans Control Syst Technol 2014;22(3):955–66. https://doi.org/10.1109/TCST.2013.2266662.
[15] Lü F, Chen H, Fan C, Chen S. A novel control algorithm for weld pool control. Ind Rob 2010;37(1):89–96. https://doi.org/10.1108/01439911011009993.
[16] Erden MS, Marić B. Assisting manual welding with robot. Robot Comput Integr Manuf 2011;27(4):818–28. https://doi.org/10.1016/j.rcim.2011.01.003.
[17] Popović O, Prokić-Cvetković R, Burzić M, Lukić U, Beljić B. Fume and gas emission during arc welding: Hhazards and recommendation. Renew Sustain Energy Rev 2014;37:509–16. https://doi.org/10.1016/j.rser.2014.05.076.
[18] Hariri A, Leman AM, Yusof MZM, Paiman NA, Noor NM. Preliminary measurement

of welding fumes in automotive plants. Int J Environ Sci Dev 2012;3(2):146–51. https://doi.org/10.7763/ijesd.2012.v3.205.
[19] Dallos J. Combating the welder shortage. 2017 Available: https://www.fabtechexpo.com/blog/2017/12/04/combating-the-welder-shortage.
[20] Li W, Gao K, Wu J, Hu T, Wang J. SVM-based information fusion for weld deviation extraction and weld groove state identification in rotating arc narrow gap MAG welding. Int J Adv Manuf Technol 2014;74(9–12):1355–64. https://doi.org/10.1007/s00170-014-6079-x.
[21] Kim JW, Na S-J. A self-organizing fuzzy control approach to arc sensor for weld joint tracking in gas metal arc welding of butt joints. Weld J 1993;72:60–6.
[22] Xu Y, Fang G, Lv N, Chen S, Jia Zou J. Computer vision technology for seam tracking in robotic GTAW and GMAW. Robot Comput Integr Manuf 2015;32:25–36. https://doi.org/10.1016/j.rcim.2014.09.002.
[23] Gu WP, Xiong ZY, Wan W. Autonomous seam acquisition and tracking system for multi-pass welding based on vision sensor. Int J Adv Manuf Technol 2013;69(1–4):451–60. https://doi.org/10.1007/s00170-013-5034-6.
[24] Mahajan A, Figueroa F. Intelligent seam tracking using ultrasonic sensors for robotic welding. Robotica 1997;15(3):275–81. https://doi.org/10.1017/s0263574797000313.
[25] Bae KY, Park JH. A study on development of inductive sensor for automatic weld seam tracking. J Mater Process Technol 2006;176(1–3):111–6. https://doi.org/10.1016/j.jmatprotec.2006.02.020.
[26] Zhu J, Wang J, Su N, Xu G, Yang M. An infrared visual sensing detection approach for swing arc narrow gap weld deviation. J Mater Process Technol 2017;243:258–68. https://doi.org/10.1016/j.jmatprotec.2016.12.029.
[27] Butler B. Tactile Seam Tracking Systems. Available: https://www.lincolnelectric.com/en-us/support/process-and-theory/pages/tactile-seam-tracking-systems.aspx.
[28] Jeong S-K, Lee G-Y, Lee W-K, Kim S-B. Development of high speed rotating arc sensor and seam tracking controller for welding robots. Proc IEEE Int Symp Ind Electron, 2. 2001. p. 845–50. https://doi.org/10.1109/ISIE.2001.931578.
[29] Shi YH, Yoo WS, Na SJ. Mathematical modelling of rotational arc sensor in GMAW and its applications to seam tracking and endpoint detection. Sci Technol Weld Join 2006;11(6):723–30. https://doi.org/10.1179/174329306x153196.
[30] Xu Y, Zhong J, Ding M, Chen H, Chen S. The acquisition and processing of real-time information for height tracking of robotic GTAW process by arc sensor. Int J Adv Manuf Technol 2013;65(5–8):1031–43. https://doi.org/10.1007/s00170-012-4237-6.
[31] Posada J, Toro C, Barandiaran I, Oyarzun D, Stricker D, De Amicis R, et al. Visual omputing as a key enabling technology for industrie 4. 0 and industrial internet. IEEE Comput Graph Appl 2015;35(2):26–40. https://doi.org/10.1109/MCG.2015.45.
[32] Qi Q, Tao F. Digital twin and Big data towards smart manufacturing and industry 4. 0: 360 degree comparison. IEEE Access 2018;6:3585–93. https://doi.org/10.1109/ACCESS.2018.2793265.
[33] Whyte J, Bouchlaghem N, Thorpe A, McCaffer R. From CAD to virtual reality: modelling approaches, data exchange and interactive 3D building design tools. Autom Constr 2000;10(1):43–55. https://doi.org/10.1016/S0926-5805(99)00012-6.
[34] Ye J, Badiyani S, Raja V, Schlegel T. Applications of virtual reality in product design evaluation. Proc Int Conf Human-Computer Interact 2007. p. 1190–9. https://doi.org/10.1007/978-3-540-73111-5_130.
[35] Berg LP, Vance JM. Industry use of virtual reality in product design and manufacturing: a survey. Virtual Real 2017;21(1):1–17. https://doi.org/10.1007/s10055-016-0293-9.
[36] Seth A, Vance JM, Oliver JH. Virtual reality for assembly methods prototyping: a review. Virtual Real 2011;15(1):5–20. https://doi.org/10.1007/s10055-009-0153-y.
[37] Noon C, Zhang R, Winer E, Oliver J, Gilmore B, Duncan J. A system for rapid creation and assessment of conceptual large vehicle designs using immersive virtual reality. Comput Ind 2012;63(5):500–12. https://doi.org/10.1016/j.compind.2012.02.003.
[38] Chellali A, Jourdan F, Dumas C. VR4D: an immersive and collaborative experience to improve the interior design process. Proc Joint Virtual Real Conf. 2013. p. 61–5.
[39] Lawson G, Herriotts P, Malcolm L, Gabrecht K, Hermawati S. The use of virtual reality and physical tools in the development and validation of ease of entry and exit in passenger vehicles. Appl Ergon 2015;48:240–51. https://doi.org/10.1016/j.apergo.2014.12.007.
[40] Lawson G, Salanitri D, Waterfield B. Future directions for the development of virtual reality within an automotive manufacturer. Appl Ergon 2016;53:323–30. https://doi.org/10.1016/j.apergo.2015.06.024.
[41] Lee WB, Cheung CF, Li JG. Applications of virtual manufacturing in materials processing. J Mater Process Technol 2001;113(1–3):416–23. https://doi.org/10.1016/S0924-0136(01)00668-9.
[42] Mujber TS, Szecsi T, Hashmi MSJ. Virtual reality applications in manufacturing process simulation. J Mater Process Technol 2004;155–156:1834–8. https://doi.org/10.1016/j.jmatprotec.2004.04.401.
[43] Roldán JJ, Crespo E, Martín-Barrio A, Peña-Tapia E, Barrientos A. A training system for industry 4. 0 operators in complex assemblies based on virtual reality and process mining. Robot Comput Integr Manuf 2019;59:305–16. https://doi.org/10.1016/j.rcim.2019.05.004.
[44] Stone RT, Watts KP, Zhong P. Virtual reality integrated welder training. Weld J 2011;90(7):136–41.
[45] Bal M, Hashemipour M. Virtual factory approach for implementation of holonic control in industrial applications: a case study in die-casting industry. Robot Comput Integr Manuf 2009;25(3):570–81. https://doi.org/10.1016/j.rcim.2008.03.020.
[46] Lee GA, Yang U, Son W, Kim Y, Jo D, Kim KH, et al. Virtual reality content-based training for spray painting tasks in the shipbuilding industry. ETRI J 2010;32(5):695–703. https://doi.org/10.4218/etrij.10.1510.0105.
[47] Goulding J, Nadim W, Petridis P, Alshawi M. Construction industry offsite production: a virtual reality interactive training environment prototype. Adv Eng Informatics 2012;26(1):103–16. https://doi.org/10.1016/j.aei.2011.09.004.
[48] Zhang H. Head-mounted display-based intuitive virtual reality training system for the mining industry. Int J Min Sci Technol 2017;27(4):717–22. https://doi.org/10.1016/j.ijmst.2017.05.005.
[49] Ning J, Sievers DE, Garmestani H, Liang SY. Analytical modeling of transient temperature in powder feed metal additive manufacturing during heating and cooling stages. Appl Phys A Mater Sci Process 2019;125(8):496. https://doi.org/10.1007/s00339-019-2782-7.
[50] Ning J, Mirkoohi E, Dong Y, Sievers DE, Garmestani H, Liang SY. Analytical modeling of 3D temperature distribution in selective laser melting of Ti-6Al-4V considering part boundary conditions. J Manuf Process 2019;44:319–26. https://doi.org/10.1016/j.jmapro.2019.06.013.
[51] Ning J, Sievers D, Garmestani H, Liang S. Analytical of in-process temperature in powder bed additive manufacturing considering laser power absorption, latent heat, scanning strategy, and powder packing. Materials (Basel) 2019;12:808. https://doi.org/10.3390/ma12050808.
[52] Li F, Ning J, Liang SY. Analytical modeling of the temperature using uniform moving heat source in planar induction heating process. Appl Sci 2019;9(7):1445. https://doi.org/10.3390/app9071445.